Potential Beneficial Metabolic Interactions Between Tamoxifen and Isoflavones via Cytochrome P450–Mediated Pathways in Female Rat Liver Microsomes

Jun Chen,[1] Steven C. Halls,[2] Joshua F. Alfaro,[2] Zhaohui Zhou,[2] and Ming Hu[1,3]

Received January 17, 2004; accepted July 14, 2004

Purpose. This study aims to evaluate a cytochrome P450–based tamoxifen-isoflavone interaction and to determine the mechanisms responsible for inhibitory effects of isoflavones (e.g., genistein) on the formation of α-hydroxytamoxifen.

Methods. Metabolism studies were performed *in vitro* using female rat liver microsomes. The effects of genistein and an isoflavone mixture on tamoxifen metabolism and the inhibition mechanism were determined using standard kinetic analysis, preincubation, and selective chemical inhibitors of P450.

Results. Metabolism of tamoxifen was saturable with K_m values of 4.9 ± 0.6, 14.6 ± 2.2, 25 ± 5.9 μM and V_{max} values of 34.7 ± 1.4, 297.5 ± 19.2, 1867 ± 231 pmol min^{-1} mg^{-1} for α-hydroxylation, *N*-desmethylation, and *N*-oxidation, respectively. Genistein (25 μM) inhibited α-hydroxylation at 2.5 μM tamoxifen by 64% ($p < 0.001$) but did not affect the 4-hydroxylation, *N*-desmethylation, and *N*-oxidation. A combination of three (genistein, daidzein, and glycitein) to five isoflavones (plus biochanin A and formononetin) inhibited tamoxifen α-hydroxylation to a greater extent but did not decrease the formation of identified metabolites. The inhibition on α-hydroxylation by genistein was mixed-typed with a K_i value of 10.6 μM. Studies using selective chemical inhibitors showed that tamoxifen α-hydroxylation was mainly mediated by rat CYP1A2 and CYP3A1/2 and that genistein 3′-hydroxylation was mainly mediated by rat CYP1A2, CYP2C6 and CYP2D1.

Conclusions. Genistein and its isoflavone analogs have the potential to decrease side effects of tamoxifen through metabolic interactions that inhibit the formation of α-hydroxytamoxifen via inhibition of CYP1A2.

KEY WORDS: cytochrome P450; drug interaction; genistein; rat liver microsomes; tamoxifen.

INTRODUCTION

Tamoxifen, the most prescribed drug for cancer treatment, is also used as a chemopreventive agent for women with a high risk of developing breast cancer (1). Additionally, tamoxifen can treat other hormone-related cancers such as ovarian (2) and refractory prostate cancers (3). However, tamoxifen increases the incidence of endometrial cancer in women (1,4,5) and causes liver cancer in rats (6). DNA adduct formation with tamoxifen metabolites is hypothesized to be one of the likely reasons for endometrial cancer (6), but tissue specific proliferative effects of tamoxifen and its metabolites may also be the causes (1,7). A minor metabolite of tamoxifen (Scheme 1), α-hydroxytamoxifen, and its sulfate are thought to be responsible for DNA adducts formation (8,9). In contrast, major metabolites of tamoxifen such as 4-hydroxytamoxifen and *N*-desmethyltamoxifen (Scheme 1) are at least as active as tamoxifen but are not known to cause cancer (6,10).

Tamoxifen undergoes extensive phase I metabolism to form numerous metabolites (see Scheme 1 for major ones) *in vivo* (11–13) and *in vitro* (14–16). Tamoxifen metabolism is mainly mediated via P450-catalyzed biotransformation processes. Tamoxifen α-hydroxylation is primarily catalyzed by CYP3A in human hepatic microsomes (16), whereas 4-hydroxy, *N*-desmethyl, and *N*-oxide metabolites of tamoxifen are mainly formed by the action of CYP2D6, CYP3A4, and flavin-containing monooxygenase (FMO), respectively (14,17).

Genistein, an isoflavone, is the main component of soy isoflavones that may exert a variety of health benefits. The claimed benefits include reduction of cancer risk, relief of postmenopausal symptoms, and maintenance of cardiovascular health (18–21). Genistein undergoes extensive phase I (CYP mediated) and phase II (UDP-glucuronosyltransferases and sulfotransferases mediated) metabolisms in intestine and liver, resulting in low bioavailability (22–27). Several oxidized metabolites of genistein have been isolated from human plasma (24,26,28). Total plasma concentrations of isoflavones can reach low micromolar range (1–5 μM), after a consumption of soy rich food or soy isoflavone supplement (22–24).

Postmenopausal women are increasing their consumption of isoflavone-containing products, particularly as the result of failed hormone replacement therapy (HRT) trial. For breast cancer survivors, the need for an alternative is more urgent. As a consequence, more than 50% of them use alternative medicine for HRT (29), and isoflavones is one of their favorable choices (30–32). Breast cancer survivors may have a higher chance of using isoflavones as HRT because tamoxifen increases the incidence of hot flashes (1).

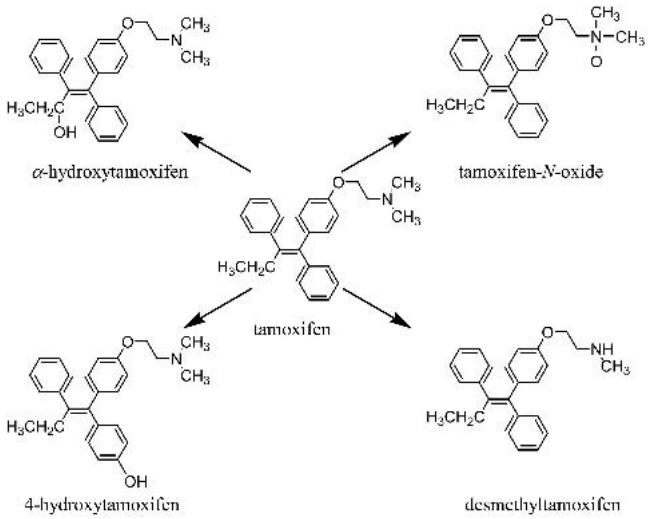

Scheme 1. Tamoxifen and some of its metabolites *in vivo*.

[1] Department of Pharmaceutical Sciences, College of Pharmacy, Washington State University, Pullman, Washington 99164, USA.
[2] Department of Chemistry, Washington State University, Pullman, Washington 99164, USA.
[3] To whom correspondence should be addressed. (e-mail: minghu@wsu.edu)

A combination of tamoxifen and isoflavones may be desirable because they have synergistic antiproliferative and cytotoxic actions against breast cancer (33,34). However, studies concerning their metabolic interactions have not been reported, and whether genistein would favorably or adversely affect the metabolism of tamoxifen is unknown. Hence, the main objectives of this study were to 1) evaluate the phase I metabolism of tamoxifen in female rat liver microsomes, 2) investigate the influence of genistein and its analogs on the formation of active or toxic metabolites of tamoxifen, 3) explore the mechanisms of their possible interactions, and 4) provide useful mechanistic information describing which P450 isoforms may be involved in potential metabolic interactions between tamoxifen and isoflavones.

MATERIALS AND METHODS

Materials

Tamoxifen, 4-hydroxytamoxifen, NADP, glucose-6-phosphate sodium, glucose-6-phosphate dehydrogenase, and P450 chemical inhibitors or substrates (α-naphthoflavone, furafylline, sulfaphenazole, quinidine, tranylcypromine, lovastatin, indomethacin, ketoconazole, troleandomycin, and quercetin) were bought from Sigma Chemical Co. (St. Louis, MO, USA). SK&F525 was obtained from SmithKline Laboratories (Philadelphia, PA, USA). Tamoxifen metabolite standards: α-hydroxy and *N*-desmethyl tamoxifen were kindly provided by Dr. Fredric Beland of FDA (Little Rock, AK, USA) and Dr. Judy Bolton of University of Illinois (Chicago, IL, USA). Tamoxifen-*N*-oxide was synthesized (see Appendix). Genistein, daidzein, glycitein, biochanin A, and formononetin were purchased from Indofine Chemicals (Wayne, NJ, USA). 3′-Hydroxygenistein was synthesized as described (25). HPLC grade acetonitrile and methylene chloride were purchased from Fisher Scientific (Pittsburgh, PA, USA). Other materials were used as received.

Rat Liver Microsomes Preparation

Female rat liver microsomes (FRLM) were prepared from adult female Sprague-Dawley rats (200~250 g) using a procedure adopted from the literature with minor modification (35). Briefly, eight fresh rat livers were harvested from euthanized rats using a procedure approved by Washington State University's Institutional Animal Care and Uses Committee. The livers were perfused with and washed with ice-cold saline, weighed and minced. Minced livers were homogenized using a motorized homogenizer (4 strokes) in ice-cold homogenization buffer (50 mM potassium phosphate, 250 mM sucrose, 1 mM EDTA, pH 7.4) and centrifuged at 7700 × *g* for 15 min at 4°C. The supernatant collected was then centrifuged again at 18,500 × *g* for 15 min at 4°C. After the pellet was discarded, the supernatant was centrifuged again at 85,600 × *g* for 1 h at 4°C to yield microsomal pellets. The microsomes were resuspended in washing buffer (10 mM potassium phosphate, 0.1 mM EDTA, 150 mM KCl, pH 7.4), and re-pelleted by centrifugation at 85,600 × *g* for 1 h at 4°C to yield microsomes. The microsomal pellets were then resuspended in 250 mM sucrose, aliquoted into vials (0.5 ml per vial) and stored at –80°C until use. The concentration of microsomal protein (normally 25–35 mg/ml) was determined by the Bio-Rad protein assay (Bio-Rad laboratories, Hercules, CA, USA) using bovine serum albumin as the standard.

Microsomal Metabolism Experiments

Microsomes were incubated at 37°C with a NADPH regenerating system and different concentrations of a substrate with or without a potential inhibitor at a selected concentration for 20 min in a 100 mM pH 7.4 potassium phosphate buffer as described previously (25). The reaction was terminated at the end of an incubation period, and 6-hydroxytestesterone (2.5 nmol, used as the internal standard) was added. Tamoxifen and its metabolites were extracted with 8 ml methylene chloride, where was then evaporated, and the dried samples were reconstituted in 50% (v/v) methanol for HPLC analysis. When tamoxifen samples were processed in the presence of isoflavones, 0.5 ml of 1 M NaOH was added to each sample thereby ensuring that isoflavones and their metabolites would not be extracted into methylene chloride, since preliminary studies showed that some of the isoflavones and/or their metabolites interfered with the quantification of tamoxifen metabolites (not shown). In genistein metabolism experiments, the experimental conditions were the same as described previously (25).

HPLC Analysis

The metabolic samples were examined by HPLC using an Agilent 1090 system, running ChemStation software, which consisted of a quaternary pump, a photodiode array detector and an autosampler (Wilmington, DE, USA). Extracted metabolites were separated using a C18 column (Aqua 5 μm, 150 × 4.6 mm; Phenomenex, Torrance, CA, USA) at a flow rate of 1 ml/min. Tamoxifen and its metabolites were monitored at 244 and 210 nm and eluted with a gradient method (0–18 min, mobile phase A 25–43%, linear gradient; 18–24 min, 43% mobile phase A; 24–28 min, mobile phase A 43–49%, linear gradient; 28–38 min, mobile phase A 49–69%, linear gradient; 38–41 min, 25% mobile phase A) using mobile phase A (100% acetonitrile) and mobile phase B (pH 3.0 potassium phosphate buffer 50 mM). A re-equilibrium time of 5 min was allowed between injections. Under this condition, the retention time for α-hydroxytamoxifen, 4-hydroxytamoxifen, *N*-desmethyltamoxifen, tamoxifen-*N*-oxide, and tamoxifen were 12.7, 19.4, 27.9, 34.0, and 29.2 min, respectively. The internal standard 6-hydroxytestosterone had a retention time of 7.1 min (Fig. 1A).

Identification of Tamoxifen Metabolites by Tandem Mass Spectrometry

Dried samples were dissolved in 50% methanol and applied to the same chromatographic conditions described above for HPLC analysis of metabolites, with the following modifications: the mobile phase contained 1% formic acid rather than a phosphate buffer and an Agilent 1100 HPLC system (Waldbronn, Germany) with binary pump, autosampler, and UV detector. The effluent was introduced into an API 4000 mass spectrometer (Applied Biosystems, Foster City, CA, USA) using turbo ion spray. Ionization and fragmentation parameters (collision energy 30 V) were optimized using a tamoxifen standard infused into a constant flow (1 ml/min) of 1% (v/v) formic acid in H_2O: acetonitrile (3:1 v/v).

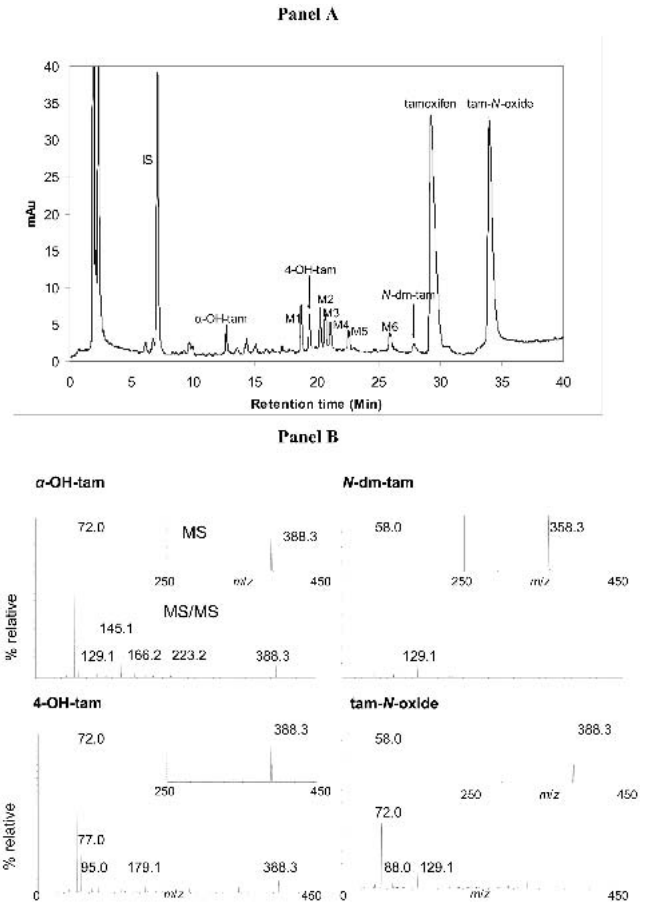

Fig. 1. HPLC chromatogram of tamoxifen metabolism in female rat liver microsomes (FRLM) (panel A) and tandem mass spectra of tamoxifen metabolites (panel B). Method used to generate these chromatograms was described under "Microsomal Metabolism Experiment." Briefly, microsomes were incubated with 10 μM tamoxifen for 20 min at 37°C in the presence of a NADPH regenerating system. Tamoxifen metabolites were extracted with methylene chloride, and then dried. Dried samples were reconstituted by 50% (v/v) methanol/water and analyzed by HPLC. There were 10 new peaks from the HPLC chromatogram and they were labeled as α-OH-tam (α-hydroxytamoxifen), 4-OH-tam (4-hydroxytamoxifen), *N*-dm-tam (*N*-desmethyltamoxifen), tam-*N*-oxide (tamoxifen-*N*-Oxide), and unknown metabolites M1-M6. We used 6-hydroxytestesterone (2.5 nmol) as the internal standard, which was added prior to extraction. Panel B presents the tandem mass spectra of standard α-hydroxyl, 4-hydroxyl, *N*-desmethyl, and *N*-oxide of tamoxifen. Insets show the mass spectra of the parent ion used to generate the product ion spectra.

The effluent was monitored for a total MS and product (MS/MS) of the most intense parent ions in both positive and negative mode.

Identification of Genistein and 3′-Hydroxygenistein

These two compounds were monitored at 254 and 220 nm, and eluted with gradient method as described (25), generating the HPLC chromatogram shown in Fig. 2.

Kinetic Analysis of Tamoxifen Metabolism

The initial rates (V) of α-hydroxytamoxifen, 4-hydroxytamoxifen, *N*-desmethyltamoxifen, and tamoxifen-*N*-oxide formation were obtained at different tamoxifen concentrations (C) of 1, 2, 4, 8, 12, 20, and 40 μM. The apparent K_m (Michaelis constant) and V_{max} (maximum reaction rate) values were estimated using a packaged nonlinear regression analysis method (SigmaPlot, SPSS Science, Chicago, IL, USA) and the Michaelis-Menten model:

$$V = \frac{V_{\max} \times C}{K_m + C} \quad (1)$$

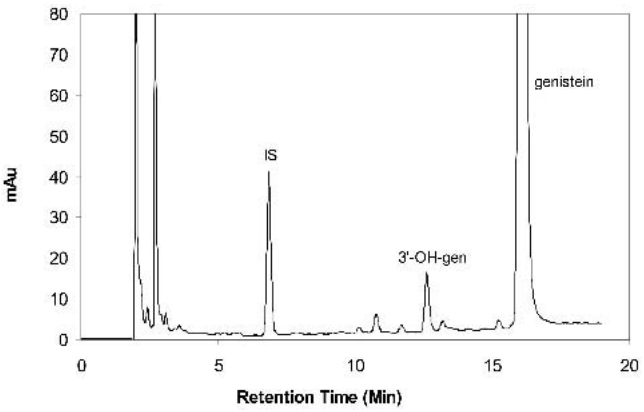

Fig. 2 HPLC chromatogram of genistein metabolism in female rat liver microsomes (FRLM). Method was described under "Microsomal Metabolism Experiment." Microsomes were incubated with 25 μM genistein for 45 min at 37°C in the presence of a NADPH regenerating system. Genistein metabolites were extracted with methylene chloride, and solvent was evaporated. Dried samples were reconstituted by 50% (v/v) methanol and analyzed by HPLC. 3′-Hydroxygenistein was the major new peak identified by its retention time in comparison with a synthesized chemical standard. The compound 7-hydroxycoumarin (10 nmol) was used as the internal standard.

Analysis of Inhibition of Tamoxifen Metabolism by Genistein

Four concentrations (C) of tamoxifen (1.25, 2.5, 5.0, 10 μM) and four concentrations (I) of genistein (0, 12.5, 18.75, 25 μM) were used to determine the mode of inhibition. A slope was obtained from the Lineweaver-Burk plot (36) for each of the genistein concentrations. The apparent K_i value (the equilibrium dissociation constant for enzyme–inhibitor complex) was obtained from the x-intercept of a plot of slope vs. inhibitor concentrations using the following equation (36):

$$\text{Slope} = \left(\frac{K_m}{V_{\max}} \times \frac{1}{K_i}\right) + \frac{K_m}{V_{\max}} \times I \quad (2)$$

The K_i values were calculated by linear regression using Microsoft Excel program.

Statistical Analysis

One-way ANOVA or unpaired Student's t test was used to analyze the data. The prior level of significance was set at 5% or $p < 0.05$.

RESULTS

Preliminary Studies

Effects of time of incubation and amounts of microsomes used in incubation were determined to optimize tamoxifen

microsomal metabolism experiments. The results indicated that an incubation time of 20 min and a microsomal concentration of 0.15 mg/ml are the best for the present study and were used subsequently unless otherwise specified. A microsomal concentration of 0.4 mg/ml was occasionally used to maintain analytical sensitivity in inhibition studies, but more microsomes were not used since higher concentration of protein did not always lead to higher metabolism (37).

Identification of Tamoxifen Metabolites

We identified known tamoxifen metabolites for the purpose of showing similarities and differences between metabolism in rat and human microsomes. Tamoxifen metabolites found in FRLM incubation were determined to be similar to those identified previously in humans and rats (14,38,39). At an initial tamoxifen concentration of 10 μM, more than 10 new metabolites peaks were found in the HPLC chromatogram (Fig. 1A). The known metabolites of tamoxifen were labeled as α-hydroxytamoxifen (m/z = 388.3, $[M+H]^+$), 4-hydroxytamoxifen (m/z = 388.3, $[M+H]^+$), *N*-desmethyltamoxifen (m/z = 358.3, $[M+H]^+$) and tamoxifen-*N*-oxide (m/z = 388.3, $[M+H]^+$), which were identified by their retention times in comparison with authentic standards and confirmed by LC/MS/MS (Fig. 1B). In addition to the above four metabolites, several other metabolites were detected by LC/MS/MS. However, specific assignments for these metabolites were not made, as metabolite identification was not the focus of the current study. Formation rates of α-hydroxy, 4-hydroxy, *N*-desmethyl, and *N*-oxide metabolites of tamoxifen were 22.9 ± 0.8, 80.8 ± 3, 126 ± 10, and 559 ± 33.4 pmol min^{-1} mg^{-1} of microsomal protein, respectively. Tamoxifen-*N*-oxide formation rate was the most rapid, whereas α-hydroxytamoxifen formation was the slowest among the identified metabolites.

Identification of Genistein Metabolites

The compound 3′-hydroxygenistein was identified as the major phase I metabolite in FRLM incubation (Fig. 2), using an authentic synthetic standard. The formation rate of 3′-hydroxygenistein (@25 μM genistein) was 84.5 ± 3.4 pmol min^{-1} mg $protein^{-1}$. The formation of 3′-hydroxygenistein increased linearly with time ($p < 0.001$) for up to an hour, and the formation rate also increased linearly with microsome amounts for up to 0.9 mg/ml (data not shown). Therefore, subsequent studies of genistein metabolism used 0.4 mg/ml microsomal protein and a 45 min incubation time.

Determination of Kinetic Parameters of Tamoxifen Metabolism

We examined formation rates of four known metabolites of tamoxifen as a function of tamoxifen concentration (1–40 μM) (Fig. 3), in order to determine kinetic descriptors of CYP-catalyzed metabolism. The results indicated that the rates were dependent upon tamoxifen concentration with apparent K_m values of 4.9 ± 0.6, 14.6 ± 2.2, 25 ± 5.9 μM, and apparent V_{max} values of 34.7 ± 1.4, 298 ± 19, 1867 ± 231 pmol min^{-1} mg $protein^{-1}$ for α-hydroxy, *N*-desmethyl, and *N*-oxide metabolites of tamoxifen (Figs. 3A, 3C, and 3D), respectively (Table I). The relationship between the formation rate of 4-hydroxytamoxifen and tamoxifen concentration was more complex, which prevented determination of its kinetic parameters using a simple Michaelis-Menten model (Fig. 3B). Eadie-Hoffstee plots generated suggested the dominance of more than one isoform in the formation of all the metabolites except *N*-desmethyltamoxifen, which appeared to have one dominant form.

Effect of Genistein and Its Analogs on Tamoxifen Metabolite Formation

To determine possible metabolic interactions between genistein and tamoxifen, we measured the formation rates of four known metabolites of tamoxifen (2.5 μM) in the presence of increasing concentrations of genistein (Fig. 4A). The results indicated that formation rate of α-hydroxytamoxifen decreased (maximum = 64%) when the genistein concentration increased (maximum = 50 μM). The inhibition was concentration-dependent, and reached the maximum at 25 μM. In contrast, increasing genistein concentration did not affect ($p > 0.1$) the formation rates of 4-hydroxy ($p > 0.05$), *N*-desmethyl ($p > 0.1$), and *N*-oxide ($p > 0.1$) metabolites of tamoxifen.

We also determined the effect of several isoflavone combinations since popular soy and herbal supplements always contain a mixture of these isoflavones. The results indicated that a mixture of three soy isoflavones (genistein, daidzein, and glycitein at 5 and 10 μM each) inhibited α-hydroxytamoxifen formation by 36% ($p < 0.001$) and 46% ($p < 0.001$), respectively (Fig. 4B). A mix of five isoflavones (genistein, daidzein, glycitein, biochanin A, and formononetin at 5 and 10 μM each), which are contained in popular red clover extracts, inhibited α-hydroxytamoxifen formation by more than 60% (Fig. 4B). Similar to the effects of genistein, formation rates of active tamoxifen metabolites such as 4-hydroxytamoxifen and tamoxifen-*N*-oxide were not altered.

We also determined the effect of these isoflavones on the formation of 6-hydroxy-testosterone, a typical CYP3A-catalyzed reaction. The results indicated that 200 μM of genistein, formononetin, daidzein, and prunetin did not inhibit the metabolism of testosterone (20 μM) to 6-hydroxy-testosterone (not shown).

Mode of Inhibition of α-Hydroxytamoxifen Formation by Genistein

To reveal the type of metabolism involved, the data were graphed using a classic Lineweaver-Burk plot (36). This was determined by using four concentrations of tamoxifen and four concentrations of genistein. The results indicated that formation rate of α-hydroxytamoxifen decreased as genistein concentration increased (Fig. 5A). The Lineweaver-Burk plots revealed that the lines did not intercept at the x- or y-axis, suggesting that the inhibition was mix-typed or partially competitive (36). The apparent K_i was 10.6 μM according to linear regression.

Absence of Mechanism-based Inhibition of α-Hydroxytamoxifen Formation by Genistein

Mechanism-based inhibition often displayed time-dependence as the result of enzyme inactivation by an inhibitor. Therefore, formation rates of α-hydroxytamoxifen (10 and 20 μM) were determined in microsomes preincubated

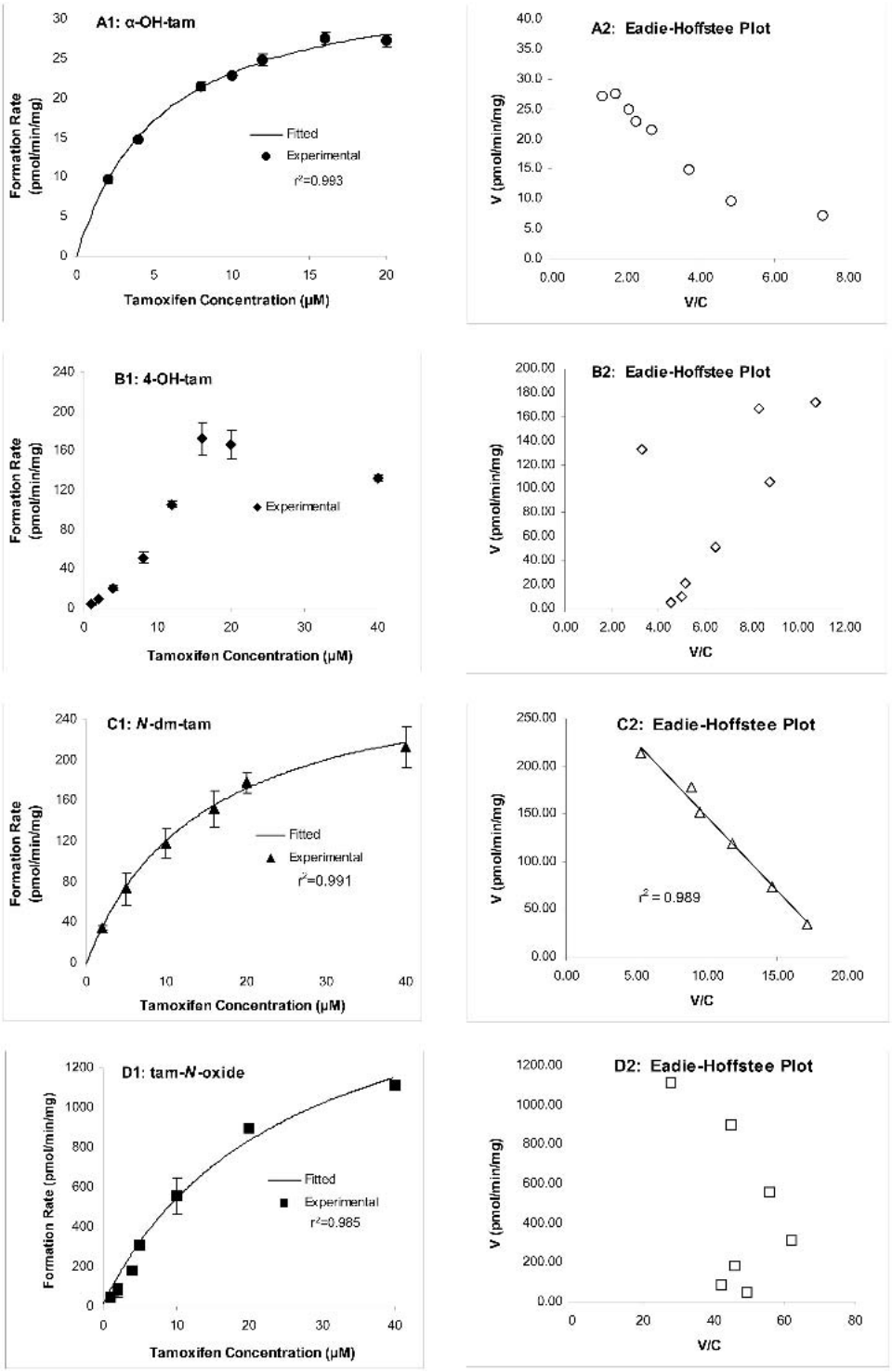

Fig. 3 Kinetic characterization of tamoxifen metabolism catalyzed by female rat liver microsomes using conventional (i.e., rate vs. concentration) plots and eadie-hoffstee plots. Formation rates of α-hydroxy (A), 4-hydroxy (B), *N*-desmethyl (C), and *N*-oxide (D) metabolites of tamoxifen were determined as described under "Materials and Methods." Each point is the average of three determinations (labeled as "Investigated") and error bars are standard deviations of the mean. The solid curve (labeled as "Estimated") in Fig.3 were fitted using K_m and V_{max} values listed in Table I.

with genistein (25 μM) for different length of time. The results indicated that preincubation with genistein for an increasing length of time (zero to 30 min) did not significantly ($p > 0.2$) increase the extent of its inhibitory effect on the formation of α-hydroxytamoxifen.

Effects of Various Prototypical Inhibitors of Cytochrome P450 Isoforms on Tamoxifen Metabolism

Prototypical selective inhibitors were used to determine which CYP isoform(s) contributes to the metabolism of

Table I. Enzyme Kinetic Parameters of Tamoxifen Metabolism in Female Rat Liver Microsomes

Apparent parameter	α-hydroxy-tamoxifen	*N*-desmethyl-tamoxifen	Tamoxifen-*N*-oxide
K_m (μM)	4.9 ± 0.6	14.6 ± 2.2	25 ± 5.9
V_{max} (pmol min^{-1} mg^{-1})	34.7 ± 1.4	298 ± 19	1867 ± 231
V_{max}/K_m (μl min^{-1} mg^{-1})[a]	6.6	20	75

[a] This ratio is commonly known as "intrinsic clearance." It is the rate constant at a substrate concentration that is substantially less than the K_m value.

tamoxifen. In order to get the maximum possible inhibition for each of the isoforms, the final inhibitor concentrations in the reaction mixtures were usually much higher than reported K_i values. The concentrations were 50 μM for SKF-525A (general P450 inhibitor) (40,41), diethyldithiocarbamic acid (CYP2E1 inhibitor) (42,43), troleandomycine (CYP3A2 inhibitor) (42), and indomethacin (CYP3A2 inhibitor) (44); 25 μM for α-naphthoflavone (CYP1A2 inhibitor) (41), quercetin, sulfaphenazole (CYP2C6 inhibitor) (43,45), lovastatin (CYP3A substrate in rat) (46), and tranylcypromine (CYP2C11 inhibitor) (41,47); and 5 μM for quinidine (CYP2D1 inhibitor) (41,45) and 2 μM for ketoconazole (CYP3A2 inhibitor) (43,45).

SKF-525A is a commonly used classic noncompetitive inhibitor for all cytochrome P450s (40,41). Its use resulted in 89%, 100%, and 53% inhibition of the formation of α-hydroxy, 4-hydroxy, and *N*-desmethyl metabolites of tamoxifen, respectively. However, SKF-525A did not inhibit the formation of tamoxifen-*N*-oxide, which was the reason we did not follow the formation of tamoxifen-*N*-oxide further.

The formation of α-hydroxytamoxifen was inhibited significantly ($p < 0.05$) by α-naphthoflavone (67%), lovastatin (58%), tranylcypromine (55%), quinidine (55%), ketoconazole (68%), troleandomycin (38%), and indomethacin (42%), but was not inhibited by sulfaphenazole and diethyldithiocarbamic acid (Table II). The extent of inhibition by quercetin was not obtained because of an unexpected interference to the measurement of α-hydroxytamoxifen by HPLC.

The formation of 4-hydroxytamoxifen was also inhibited significantly ($p < 0.05$) by α-naphthoflavone (62%), quercetin (61%), tranylcypromine (75%), quinidine (90%), ketoconazole (83%), sulfaphenazole (37%), troleandomycin (55%), and indomethacin (57%), respectively (Fig. 7B). Similar to inhibition of 4-hydroxytamoxifen formation, *N*-desmethyltamoxifen formation was significantly inhibited by α-naphthoflavone (67%), quercetin (49%), tranylcypromine (28%), indomethacin (49%), quinidine (27%), ketoconazole (59%), and troleandomycin (31%), respectively (Table II).

To characterize further the contributions of various CYP isoforms, combinations of chemical inhibitors (α-naphthoflavone 25 μM, quinidine 5 μM, tranylcypromine 25 μM and ketoconazole 2 μM) were used to determine their effect on tamoxifen metabolism. The results indicated that α-naphthoflavone inhibited α-hydroxylation by 67%. The addition of quinidine and/or tranylcypromine did not further significantly decrease the formation of α-hydroxytamoxifen. However, the addition of ketoconazole further inhibited α-hydroxylation by 50% ($p < 0.05$). Therefore, the use of these four inhibitors

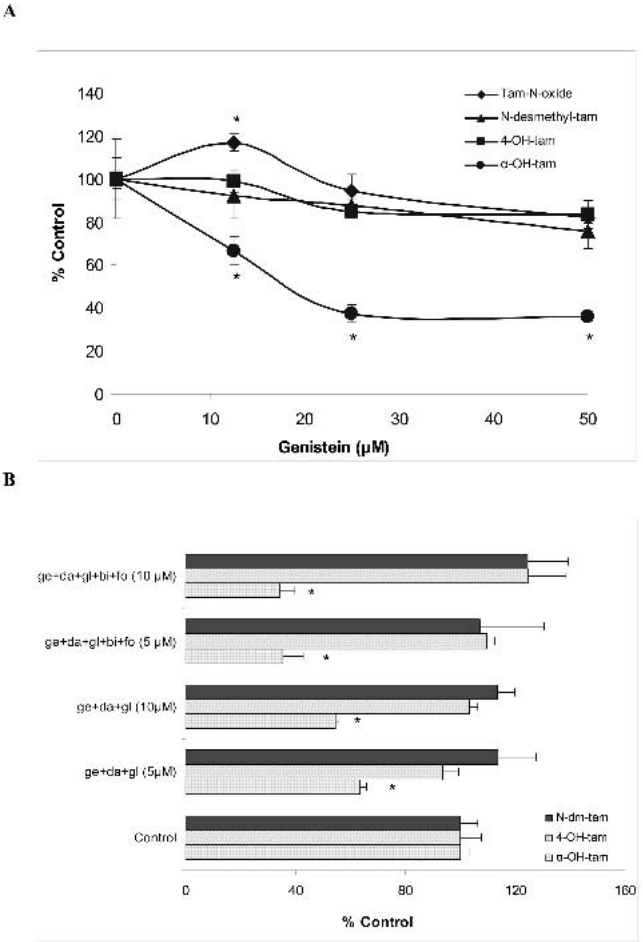

Fig. 4 Effect of genistein (A) and isoflavone mixture (B) on the formation of tamoxifen metabolites. Tamoxifen (2.5 μM) was incubated with microsomes and the NADPH regenerating system in the presence of 12.5, 25, 50 μM genistein or an isoflavones mixture at 5 or 10 μM each. A mixture of genistein (ge), daidzein (da), and glycitein (gl) are present in soy products. A mixture of three soy isoflavones plus biochanin A (bi) and formononetin (fo) are normally present in popular isoflavone extract products such as red clover. Controlled experiments used same volume and concentration of organic solvent in the place of genistein. Formation rates of α-hydroxy, 4-hydroxl, *N*-desmethyl, and *N*-oxide of tamoxifen were determined as described under "Materials and Methods." Each point or column represents mean percent control of three formation rates of these four metabolites and the error bars are standard deviations of the mean. The control values (±SD) for the formation rates of α-hydroxy, 4-hydroxy, *N*-desmethyl, and *N*-oxide metabolites of tamoxifen (at 1.25, 2.5, 5 and 10 μM of tamoxifen) were 25.7 ± 0.01, 72.7 ± 7.2, 146 ± 27, and 274 ± 11 pmol min^{-1} mg protein^{-1}, respectively.

together decreased the formation of α-hydroxytamoxifen by 80% ($p < 0.05$) (Table II).

For tamoxifen 4-hydroxylation, the use of combinatorial chemicals inhibitors (α-naphthoflavone, quinidine, tranylcypromine and ketoconazole) resulted in total of 90% ($p < 0.05$) inhibition (Table II). All these four inhibitors contributed to the maximal inhibitory effects. Last, the same combinatorial approach generated a 73% ($p < 0.05$) decrease in *N*-demethylation, and the inhibition appeared to be primarily contributed by α-naphthoflavone (Table II) because it alone inhibited the metabolism by more than 62%.

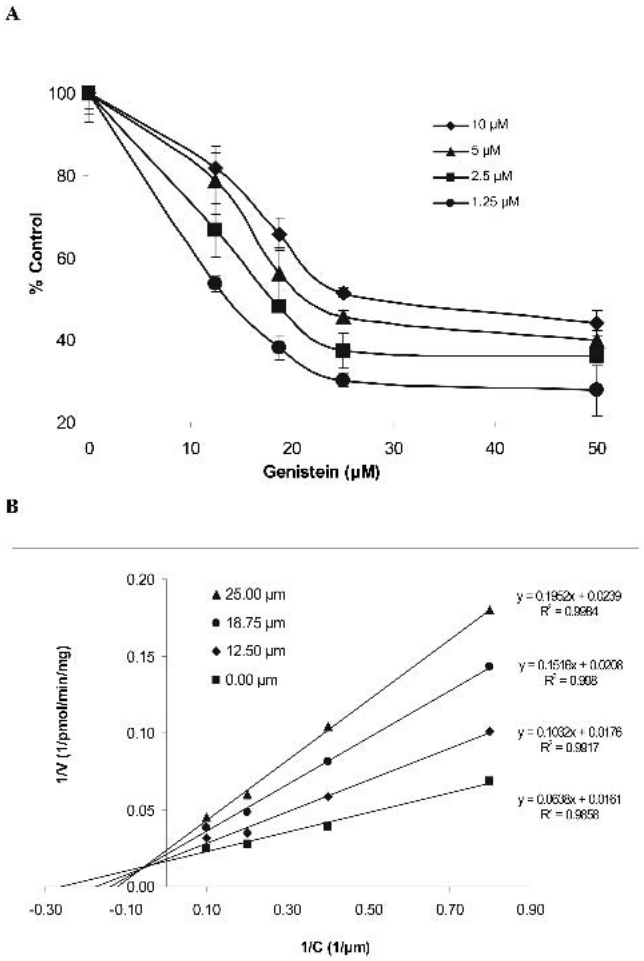

Fig. 5 Inhibition of α-hydroxytamoxifen formation by increasing concentrations of genistein (A). The Lineweaver-Burk plot is used here to determine the inhibitory mechanism by which genistein inhibits the formation of α-hydroxytamoxifen or mode of inhibition (B). Four concentrations of tamoxifen (1.25, 2.5, 5, and 10 μM) were incubated with microsomes and the NADPH regenerating system in the presence of genistein (12.5, 18.75, 25, and 50 μM) respectively. Control used the same incubation with %0.25 stock solution solvent instead of genistein. Formation rate of α-hydroxytamoxifen were determined as described under "Materials and Methods." Each point represents the mean of three determinations and the error bars are the standard deviation of the mean. The mean control values (± SD) for α-hydroxylation (at 1.25, 2.5, 5, and 10 μM of tamoxifen) were 18.5 ± 1.3, 25.7 ± 0.01, 36.7 ± 1.34, 39 ± 2.1 pmol min^{-1} mg $protein^{-1}$, respectively (A). Lines in (B) were generated by linear regression.

Effects of Prototypical Chemical Inhibitors on 3′-Hydroxygenistein Formation

Tranylcypromine, an inhibitor of CYP2C11, was the most potent among all the inhibitors tested, inhibiting the formation of 3′-hydroxygenistein by 89% ($p < 0.05$). Other inhibitors also decreased the formation of 3′-hydroxygenistein and the extent of the inhibition was 46% ($p < 0.05$) for furafylline (CYP1A2 inhibitor) (43,45), 39% ($p < 0.05$) for quinidine, and 33% ($p < 0.05$) for both sulfaphenazole and ketoconazole. The extent of inhibition was similar at two tested concentrations (25 or 50 μM for inhibitors other than quinidine, which were used at 5 or 10 μM) (Fig. 6).

DISCUSSION

The goals of this study were to determine the effects of genistein and its analogs on tamoxifen metabolism and to delineate possible mechanisms of tamoxifen-isoflavone interactions using prototypical chemical inhibitors.

Our study is designed to take into account the physiologic concentrations of tamoxifen and genistein (12,24,48). *In vivo* plasma concentrations of total genistein (mostly conjugated) in humans may reach as high as 10 μM after a single dose of soy isoflavone product (24,49). Despite this, hepatic concentrations of intact isoflavones or aglycones could reach quite a high level in liver, since these isoflavones are rapidly absorbed. On the other hand, the physiologic concentrations of tamoxifen are in a low to sub-micromolar range (12). Thus, we have chosen *in vitro* concentrations of tamoxifen and genistein/isoflavones that are close to the observed *in vivo* concentrations.

The results indicated that major metabolites (e.g., 4-hydroxytamoxifen) found in human plasma were also found in our rat microsomal studies, as was the minor metabolite of interest, α-hydroxytamoxifen (Fig. 1). On the other hand, tamoxifen-*N*-oxide was found as a major metabolite in FRLM even though it was identified as a minor metabolite in other *in vitro* studies (13), perhaps due to species difference.

We also found that the formation of these metabolites was concentration-dependent (Fig. 3) with K_m values (5–25 μM, Table I) significantly higher than *in vivo* concentrations of tamoxifen (1 μM or less), suggesting the intrinsic clearance value is a better predictor of *in vivo* clearance.

Our studies also indicated that phase I metabolism of genistein in FRLM and human liver microsomes are similar with cytochrome P450-mediated formation of 3′-hydroxygenistein as the primary metabolic pathway (24–26). Additionally, O-demethylation of methylated isoflavones (e.g., biochanin A) was also similar. A major isoform responsible for the observed phase I metabolism appears to be CYP1A2 (25). Taken together, these studies using FRLM could provide clinically relevant information about metabolic interactions between tamoxifen and isoflavones, although verification in humans would be ultimately necessary.

To determine the potential interactions, we focused our studies on the effects of isoflavones on tamoxifen metabolism. The results indicated that genistein and a mixture of its analogs significantly inhibit the formation of the toxic metabolite α-hydroxytamoxifen, but did not decrease the formation of other active metabolites (e.g., 4-hydroxytamoxifen) (Fig. 4). There was also a small but significant activation of tamoxifen-*N*-oxide formation (Fig. 4A). We are excited by this discovery since this is a rare instance of a potentially beneficial drug-supplement/herbal interaction. In contrast, there are numerous literature reports that have shown adverse interactions.

We next determined the mechanisms responsible for the inhibition of α-hydroxylation of tamoxifen by genistein. The results indicated that the inhibition is concentration-dependent, and mixed-typed (both competitive and non-competitive) (Fig. 5B) (36). The results also showed that pre-incubation of FRLM with genistein (up to 30 min) did not decrease the extent of inhibition, suggesting that genistein was not a mechanism-based inhibitor (i.e., inactivator) of α-hydroxylation of tamoxifen (Fig. 6).

We used various selective inhibitors of CYP isoforms to

Table II. Effects of Various Prototypical Chemical Inhibitors on Tamoxifen Metabolism

Inhibitors			Tamoxifen (% control)[a]					
			α-hydroxyl		4-hydroxyl		N-desmethyl	
Chemicals	CYP isoform	Conc. (μM)	%	SD	%	SD	%	SD
Control			100	7.09	100	7.09	100	2.45
SKF-525	All CYP	50	12.3	1.72	0.00	0.00	47.2	2.77
α-Naphthoflavone (N)	CYP1A2	25	32.8	2.26	37.8	0.44	33.2	2.18
Quercetin	CYP2C6	25	CND[a]	6.92	38.7	1.88	50.8	4.26
Sulfaphenazole	CYP2C6	25	107.8	6.63	62.8	0.63	202.5	5.82
Lovastatin	CYP3A	25	42.2	4.05	87.1	15.2	126.1	9.58
Tranylcypromine (T)	CYP2C11	25	45.1	3.32	25.3	2.44	62.4	4.06
Indomethacin	CYP3A2	50	57.82	6.48	82.4	1.39	51.1	15.06
Quinidine (Q)	CYP2D1	5	44.7	6.69	10.1	0.67	72.8	11.87
Diethyldithiocarbamic acid	CYP2E1	50	82.4	5.07	217.6	0.29	90.1	3.32
Ketoconazole (K)	CYP3A2	2	41.9	5.10	17.5	0.88	41.4	4.41
Troleandomycin	CYP3A2	50	62.4	2.26	45.7	1.54	69.1	0.62
N + Q			35.5	0.26	28.2	8.38	78.0	2.55
N + Q + T			40.3	3.49	16.8	1.87	61.1	4.75
N + Q + T + K			19.7	0.43	9.7	0.70	26.6	1.49

CND stands for "cannot be determined" because of technical difficulty. In this case, a contamination peak from quercetin.
[a] The results are expressed as the remaining rate of metabolism after normalizing for control.

further confirm which CYP isoforms were responsible for the observed drug-isoflavone interactions. To accomplish this objective, we needed to determine CYP isoforms involved in tamoxifen and genistein metabolism separately and jointly.

We first determined the maximal contribution of different CYP isoforms to the formation of α-hydroxytamoxifen. Among these inhibitors, the CYP1A2 inhibitor α-naphthoflavone appeared to significantly decrease its formation, suggesting that CYP1A2 makes a significant contribution to α-hydroxylation of tamoxifen. The CYP3A1/2 inhibitor ketoconazole (2 μM), which is a potent CYP3A1/2 inhibitor in rat with an IC_{50} value of 0.29 μM (44), inhibited α-hydroxylation by 58%. However, at concentrations at or above 1 μM, ketoconazole also inhibits CYP2C6 (45). In this case, however, CYP2C6 was not involved since sulfaphenazole (45), the most potent and highly specific CYP2C6 inhibitor, did not cause any inhibition. Therefore, CYP3A1/2 and CYP1A2 are likely the main CYP isoforms responsible for α-hydroxylation of tamoxifen. This is supported by the facts that addition of ketoconazole to the inhibitor mixture further inhibited the formation of α-hydroxytamoxifen by 50% (Table II). Furthermore, the relationship shown in the Eadie-Hoffstee plot suggested the involvement of at least two isoforms for the formation of α-hydroxytamoxifen (Fig. 3A). Additionally, the involvement of CYP3A1/2 is supported by inhibitory action of a more specific CYP3A1/2 inhibitor, troleandomycine (41), and another CYP3A1/2 inhibitor indomethacin (Table II).

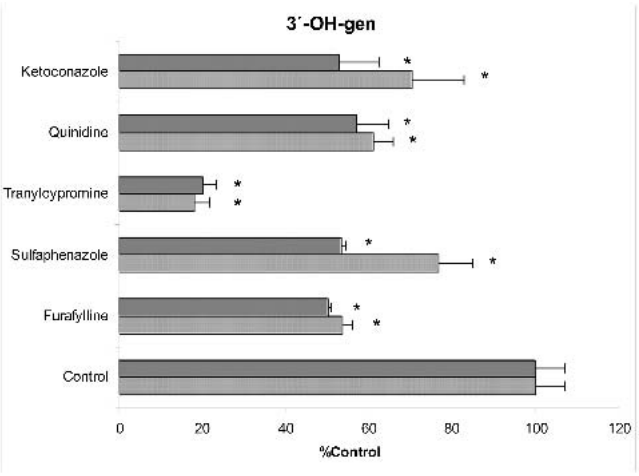

Fig. 6 Effects of selective cytochrome P450 inhibitors on genistein metabolism. Genistein (25 μM) was incubated with microsomes and the NADPH regenerating system in the presence of P450 inhibitor furafylline or sulfaphenazole or tranylcypromine or ketoconazole at concentration of 25 and 50 μM, or quinidine at 5 and 10 μM, as described. Equivalent amounts of organic solvent (0.15% in this case) were added instead of inhibitors in the control experiment. Formation rate of 3′-hydroxylgenistein (3′-OH-Gen) were determined as described under "Materials and Methods." Each column represents the mean of three determinations and the error bars are the standard deviation of the mean. The mean control value (±SD) for formation rates of 3′-hydroxylgenistein was 84.5 ± 3.4 pmol min^{-1} mg $protein^{-1}$.

Although tranylcypromine and quinidine were effective inhibitors of α-hydroxylation of tamoxifen, addition of these two compounds to the inhibitor mixture did not result in greater extent of inhibition, suggesting that the contribution of CYP2D1 and CYP2C11 is minimal (Table II). The observed inhibitory effects may be due to the cross inhibition of other CYP isoforms by these compounds. For example, quinidine, a potent CYP2D1 inhibitor in rat liver microsomes (41), also inhibited rat CYP3A1/2 and CYP2C6 at 1 μM (45).

We then determined the contribution of various CYP isoforms on the formation of 3′-hydroxygenistein. The inhibitor results suggest that CYP1A2, CYP2C6, CYP2D1 and CYP3A1/2 subfamilies could contribute to the formation of 3′-hydroxygenistein. However, the involvement of CYP3A1/2 may be small since genistein did not inhibit the formation of 6-hydroxytestosterone or 4-hydroxytamoxifen, both involving CYP3A1/2. Previously, we have shown that CYP1A and CYP2C subfamilies are involved in the 3′-hydroxylation of genistein in human liver microsomes (25).

Together, these results indicated α-hydroxylation of

tamoxifen and 3′-hydroxylation of genistein may share a few cytochrome P450 pathways. The involvement of CYP1A2 is likely since genistein could compete for the same metabolic pathways.

Finally, we would like to briefly comment on the significance of our research from a clinical point of view, since there is no information about these compounds' potential interactions in humans. We also want to point out that our studies were conducted in rat liver microsomes, which are very different from humans *in vivo*. Nevertheless, we believe that we have for the first time observed potential beneficial metabolic interactions between drugs and herbal supplements, which is rarely reported. Therefore, our discovery suggests that additional studies in humans may be warranted to determine if the combination is beneficial for patients. Another important point is that different inhibitors of CYP isoforms could potential change the nature of interactions (i.e., toxic or beneficial). That change could influence which combination of tamoxifen and prescription drugs (e.g., ketoconazole, lovastatin) or over-the-counter medications (e.g., quercetin is sold as a herbal product) is beneficial vs. harmful to the patients.

In conclusion, this study demonstrates that isoflavones decrease the formation of toxic α-hydroxytamoxifen through metabolic interactions using rat liver microsomes. The mechanism responsible for tamoxifen-genistein metabolic interactions appears to be mediated via competitive and noncompetitive inhibition of CYP1A2. Even though the potential benefit of co-administering isoflavones and tamoxifen for human remained to be demonstrated, as there is evidence that α-hydroxytamoxifen is mainly formed via the action of CYP3A4 in human microsomes, this study shows the potential for a benefit interaction between a properly chosen nutritional supplement and conventional drug.

ACKNOWLEDGMENT

This work was supported by NIH AT00182 and NIH CA 87779. We thank Dr. Fredrick Beland of FDA (Little Rock, AK) and Dr. Judy Bolton (University of Illinois) for providing metabolic standards.

REFERENCES

1. V. C. Jordan, S. Gapstur, and M. Morrow. Selective estrogen receptor modulation and reduction in risk of breast cancer, osteoporosis, and coronary heart disease. *J. Natl. Cancer Inst.* **93**: 1449–1457 (2001).
2. J. L Perez-Gracia and E. M Carrasco. Tamoxifen therapy for ovarian cancer in the adjuvant and advanced settings: systematic review of the literature and implications for future research. *Gynecol. Oncol.* **84**:201–209 (2002).
3. R. C Bergan, E. Reed, C. E Myers, D. Headlee, O. Brawley, H. K. Cho, W. D. Figg, A. Tompkins, W. M. Linehan, D. Kohler, S. M Steinberg, and M. V. Blagosklonny. A Phase II study of high-dose tamoxifen in patients with hormone-refractory prostate cancer. *Clin. Cancer Res.* **5**:2366–2373 (1999).
4. E. Pukkala, P. Kyyronen, R. Sankila, and K. Holly. Tamoxifen and toremifene treatment of breast cancer and risk of subsequent endometrial cancer: a population-based case-control study. *Int. J. Cancer* **100**:337–341 (2002).
5. S. Shibutani, A. Ravindernath, N. Suzuki, I. Terashima, and S. M. Sugarman. A. P Grollman, M. L. Pearl. Identification of tamoxifen-DNA adducts in the endometrium of women treated with tamoxifen. *Carcinogenesis* **21**:1461–1467 (2000).
6. D. H. Phillips. Understanding the genotoxicity of tamoxifen? *Carcinogenesis* **22**:839–849 (2001).
7. I. N. White. Anti-oestrogenic drugs and endometrial cancers. *Toxicol. Lett.* **120**:21–29 (2001).
8. A. Umemoto, K. Komaki, Y. Monden, M. Suwa, Y. Kanno, M. Kitagawa, M. Suzuki, C. X. Lin, Y. Ueyama, M. A. Momen, A. Ravindernath, and S. Shibutani. Identification and quantification of tamoxifen-DNA adducts in the liver of rats and mice. *Chem. Res. Toxicol* **14**:1006–1013 (2001).
9. S. Shibutani, P. M. Shaw, N. Suzuki, L. Dasaradhi, M. W. Duffel, and I. Terashima. Sulfation of alpha-hydroxytamoxifen catalyzed by human hydroxysteroid sulfotransferase results in tamoxifen-DNA adducts. *Carcinogenesis* **19**:2007–2011 (1998).
10. G. Milano, M. C. Etienne, M. Frenay, R. Khater, J. L. Formento, N. Renee, J. L. Moll, M. Francoual, M. Berto, and M. Namer. Optimized analysis of tamoxifen and its main metabolites in the plasma and cytosol of mammary tumors. *Br. J. Cancer* **55**:509–512 (1987).
11. R. R. Reddel, L. C. Murphy, and R. L. Sutherland. Effects of biologically active metabolites of tamoxifen on the proliferation kinetics of MCF-7 human breast cancer cells *in vitro. Cancer Res.* **43**:4618–4624 (1983).
12. S. M. Langan-Fahey, D. C. Tormey, and V. C. Jordan. Tamoxifen metabolites in patients on long-term adjuvant therapy for breast cancer. *Eur. J. Cancer* **26**:883–888 (1990).
13. G. K. Poon, Y. C. Chui, R. McCague, P. E. Linning, R. Feng, M. G. Rowlands, and M. Jarman. Analysis of phase I and phase II metabolites of tamoxifen in breast cancer patients. *Drug Metab. Dispos.* **21**:1119–1124 (1993).
14. C. Mani, H. V. Gelboin, S. S. Park, R. Pearce, A. Parkinson, and D. Kupfer. Metabolism of the antimammary cancer antiestrogenic agent tamoxifen. I. Cytochrome P-450-catalyzed *N*-demethylation and 4-hydroxylation. *Drug Metab. Dispos.* **21**:645–656 (1993a).
15. C. Mani, E. Hodgson, and D. Kupfer. Metabolism of the antimammary cancer antiestrogenic agent tamoxifen. II. Cytochrome P-450-catalyzed N-demethylation and 4-hydroxylation. *Drug Metab. Dispos.* **21**:657–661 (1993b).
16. D. J. Boocock, J. L. Maggs, I. N. White, and B. K. Park. α-hydroxytamoxifen, a genotoxic metabolite of tamoxifen in the rat: identification and quantification *in vivo* and *in vitro. Carcinogenesis* **20**:153–160 (1999).
17. H. K. Crewe, L. M. Notley, R. M. Wunsch, M. S. Lennard, and E. M. Gillam. Metabolism of tamoxifen by recombinant human cytochrome P450 enzymes: formation of the 4-hydroxy, 4'-hydroxy and N-desmethyl metabolites and isomerization of trans-4-hydroxytamoxifen. *Drug Metab. Dispos.* **30**:869–874 (2002).
18. M. Kurzer and X. Xu. Dietary Phytoestrogens. *Annu. Rev. Nutr.* **17**:353–381 (1997).
19. D. F. Birt, S. Hendrich, and W. Wang. Dietary agents in cancer prevention: flavonoids and isoflavonoids. *Pharmacol. Ther.* **90**: 157–177 (2001).
20. C. S. Yang, J. M. Landau, M. T. Huang, and H. L. Newmark. Inhibition of carcinogenesis by dietary polyphenolic compounds. *Annu. Rev. Nutr.* **21**:381–406 (2001).
21. H. Wiseman. The therapeutic potential of phytoestrogens. *Expert Opin. Investig. Drugs* **9**:1829–1840 (2000).
22. Y. Liu and M. Hu. Absorption and metabolism of flavonoids in the Caco-2 cell culture model and a perfused rat intestinal model. *Drug Metab. Dispos.* **30**:370–377 (2002).
23. J. Chen, H. Lin, and M. Hu. Metabolism of flavonoids via enteric recycling: role of intestinal disposition. *J. Pharmacol. Exp. Therap* **304**:1228–1235 (2003).
24. K. D. Setchell, N. M. Brown, P. Desai, L. Zimmer-Nechemias, B. E. Wolfe, W. T. Brashear, A. S. Kirschner, A. Cassidy, and J. E. Heubi. Bioavailability of pure isoflavones in healthy humans and analysis of commercial soy isoflavone supplements. *J. Nutr.* **131**: 1362S–1375S (2001).
25. M. Hu, K. Krausz, J. Chen, X. Ge, J. Q. Li, H. L. Gelboinl, and F. J. Gonzalez. Identification of CYP1A2 the main isoform for the phase I hydroxylated metabolism of genistein and a prodrug converting enzyme of methylated isoflavones. *Drug Metab. Dispos.* **31**:924–931 (2003).
26. S. E. Kulling, D. M. Honig, and M. Metzler. Oxidative metabolism of the soy isoflavones daidzein and genistein in humans *in vitro* and *in vivo. J. Agric. Food Chem.* **49**:3024–3033 (2001).
27. E. S. Roberts-Kirchhoff, J. R. Crowley, P. F. Hollenberg, and H. Kim. Metabolism of genistein by rat and human cytochrome P450s. *Chem. Res. Toxicol.* **12**:610–616 (1999).

28. S. E. Kulling, D. M. Honig, T. J. Simat, and M. Metzler. Oxidative *in vitro* metabolism of the soy phytoestrogens daidzein and genistein. *J. Agric. Food Chem.* **48**:4963–4972 (2000).
29. K. M. Newton, D. S. Buist, N. L. Keenan, L. A. Anderson, and A. Z. LaCroix. Use of alternative therapies for menopause symptoms: results of a population-based survey. *Obstet. Gynecol.* **100**: 18–25 (2002).
30. M. J. Messina and C. L. Loprinzi. Soy for breast cancer survivors: a critical review of the literature. *J. Nutr.* **131**:3095S–3108S (2001).
31. A. Brzezinski and A. Debi. Phytoestrogens: the "natural" selective estrogen receptor modulators? *Eur. J. Obstet. Gynecol. Reprod. Biol.* **85**:47–51 (1999).
32. D. Carusi. Phytoestrogens as hormone replacement therapy: an evidence-based approach. *Care Update Ob. Gyns* **7**:253–259 (2000).
33. F. Shen, X. Xue, and G. Weber. Tamoxifen and genistein synergistically down-regulate signal transduction and proliferation in estrogen receptor-negative human breast carcinoma MDA-MB-435 cells. *Anticancer Res.* **19**:1657–1662 (1999).
34. V. Tanos, A. Brzezinski, O. Drize, N. Strauss, and T. Peretz. Synergistic inhibitory effects of genistein and tamoxifen on human dysplastic and malignant epithelial breast cells *in vitro*. *Eur. J. Obstet. Gynecol. Reprod. Biol.* **102**:188–194 (2002).
35. J. R. Okita, P. J. Castle, and R. T. Okita. Characterization of cytochromes P450 in liver and kidney of rats treated with di-(2-ethylhexyl) phthalate. *J. Biochem. Toxicol.* **8**:135–144 (1993).
36. I. H. Segel. *Enzyme Kinetics: Behavior and Analysis of Rapid Equilibrium and Steady-State Enzyme Systems.* John Wiley and Sons, New York, 1975.
37. H. K. Crewe, S. W. Ellis, M. S. Lennard, and G. T. Tucker. Variable contribution of cytochromes P450 2D6, 2C9 and 3A4 to the 4-hydroxylation of tamoxifen by human liver microsomes. *Biochem. Pharmacol.* **53**:171–178 (1997).
38. C. K. Lim, Z. X. Yuan, J. H. Lamb, I. N. White, F. De Matteis, and L. L. Smith. A comparative study of tamoxifen metabolism in female rat, mouse and human liver microsomes. *Carcinogenesis* **15**:589–593 (1994).
39. C. Mani, R. Pearce, A. Parkinson, and D. Kupfer. Involvement of cytochrome P4503A in catalysis of tamoxifen activation and covalent binding to rat and human liver microsomes. *Carcinogenesis* **15**:2715–2720 (1994).
40. H. Doi, H. Iwasaki, Y. Masubuchi, R. Nishigaki, and T. Horie. Chemiluminescence associated with the oxidative metabolism of salicylic acid in rat liver microsomes. *Chem. Biol. Interact.* **140**: 109–119 (2002).
41. W. G. Chung, C. S. Park, H. K. Roh, W. K. Lee, and Y. N. Cha. Oxidation of ranitidine by isozymes of flavin-containing monooxygenase and cytochrome P450. *Jpn. J. Pharmacol.* **84**:213–220 (2000).
42. J. Schmider, D. J. Greenblatt, S. M. Fogelman, L. L. von Moltke, and R. I. Shader. Metabolism of dextromethorphan in vitro: involvement of cytochromes P450 2D6 and 3A3/4, with a possible role of 2E1. *Biopharm. Drug Dispos.* **18**:227–240 (1997).
43. V. A. Eagling, J. F. Tjia, and D. J. Back. Differential selectivity of cytochrome P450 inhibitors against probe substrates in human and rat liver microsomes. *Br. J. Clin. Pharmacol.* **45**:107–114 (1998).
44. Y. Masubuchi, E. Masuda, and T. Horie. Multiple mechanisms in indomethacin-induced impairment of hepatic cytochrome P450 enzymes in rats. *Gastroenterology* **122**:774–783 (2002).
45. K. Kobayashi, K. Urashima, N. Shimada, and K. Chiba. Selectivities of human cytochrome P450 inhibitors toward rat P450 isoforms: study with cDNA-expressed systems of the rat. *Drug Metab. Dispos.* **31**:833–836 (2003).
46. R. W. Wang, P. H. Kari, A. Y. Lu, P. E. Thomas, F. P. Guengerich, and K. P. Vyas. Biotransformation of lovastatin. IV. Identification of cytochrome P450 3A proteins as the major enzymes responsible for the oxidative metabolism of lovastatin in rat and human liver microsomes. *Arch. Biochem. Biophys.* **290**: 355–361 (1991).
47. Y. Ando, E. Fuse, and W. D. Figg. Thalidomide metabolism by the CYP2C subfamily. *Clin. Cancer Res.* **8**:1964–1973 (2002).
48. M. G. Busby, A. R. Jeffcoat, L. T. Bloedon, M. A. Koch, T. Black, K. J. Dix, W. D. Heizer, B. F. Thomas, J. M. Hill, J. A. Crowell, and S. H. Zeisel. Clinical characteristics and pharmacokinetics of purified soy isoflavones: single-dose administration to healthy men. *Am. J. Clin. Nutr.* **75**:126–136 (2002).
49. G. K. Poon, B. Walter, P. E. Lonning, M. N. Horton, and R. McCague. Identification of tamoxifen metabolites in human HepG2 cell line, human liver homogenate, and patients on long-term therapy for breast cancer. *Drug Metab. Dispos.* **23**:377–382 (1995).

Appendix: Synthesis of Tamoxifen-*N*-Oxide

An authentic tamoxifen-*N*-oxide was prepared from tamoxifen by oxidation with 3-chloroperoxybenzoic acid (mCPBA). The structure of the product obtained was confirmed by NMR analysis. For example, the chemical shift for the methyl group connected to the nitrogen atom was determined to be 3.28 ppm for tamoxifen-*N*-oxide, compared to 2.28 ppm for tamoxifen. The changes in chemical shift values are consistent with the formation of the *N*-oxide. The following is a brief description of the chemical synthesis.

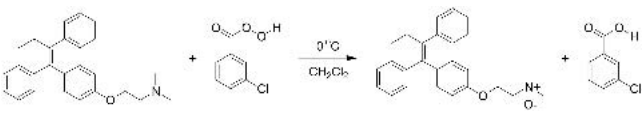

In a round-bottom flask wrapped with aluminum foil, tamoxifen (27 mg, 0.072 mmol) was dissolved in 0.5 ml of CH_2Cl_2. After the solution was cooled down to 0°C, 3-chloroperoxybenzoic acid (mCPBA) (26 mg, maximal 77%, ~0.12 mmol, dissolved in 0.25 ml of CH_2Cl_2) was added dropwise to the solution. After ~10 min, tamoxifen was completely converted to a more polar compound, as judged by thin-layer chromatography (TLC). After an additional 50 min, the reaction mixture was diluted with 40 ml of CH_2Cl_2, and was washed with a mixture of 10 ml of saturated aqueous $NaHCO_3$ and 10 ml of 10% aqueous Na_2CO_3 (final pH was 9) to remove mCPBA and 3-chlorobenzoic acid, then with brine. The organic extract was dried with $MgSO_4$ overnight (the flask was covered with aluminum foil and placed in the refrigerator). The $MgSO_4$ was filtered off and the solvent removed in vacuum. An off white solid was obtained as the desired product (22 mg, 79% yield). TLC: R_f 0.35 (Methanol). ^{1}H NMR ($CDCl_3$, 300 MHz): 0.93 (t, 3H), 2.45 (q, 2H), 3.28 (s, 6H), 3.65 (dd, 2H), 4.4 (dd, 2H), 6.55 (d, 2H), 6.78 (d, 2H), 7.08-7.26 (m, 8H), 7.27- 7.38 (m, 2H). ^{13}C NMR ($CDCl_3$, 75 MHz): 12.55, 28.01, 58.89, 60.79, 69.07, 75.59, 112.31, 125.10, 125.58, 126.90, 127.12, 128.41, 128.64, 131.02, 135.41, 136.92, 140.71, 141.22, 142.60, 154.49. DEPT: (CH): 112.31, 125.10, 125.58, 126.90, 127.12, 128.41, 128.64, 131.02; (CH_2): 28.01, 60.79, 69.07; and (CH_3): 12.56, 58.89.